

Eigenvalue Based Active User Enumeration for Grant-Free Access Under Carrier Frequency Offsets

Takanori Hara *Member, IEEE*

Abstract—This paper investigates a grant-free non-orthogonal multiple access (GF-NOMA) system in the presence of carrier frequency offsets. We propose two schemes for enumerating active users in such a GF-NOMA system, which is equivalent to estimating the sparsity level. Both schemes utilize a short common pilot and the eigenvalues of the sample covariance matrix of the received signal. The two schemes differ in their treatment of noise variance: one exploits known variance information, while the other is designed to function without this knowledge. Simulation results demonstrate the effectiveness of the proposed schemes in terms of the normalized root-mean-squared error.

Index Terms—Grant-free access, active user enumeration, sparsity level estimation, carrier frequency offsets.

I. INTRODUCTION

FUTURE wireless communication systems are required to support time-sensitive applications, such as robot control and automated driving, which involve sporadic data traffic due to massive short-packet communications [1]–[3]. The conventional multiple access schemes employing grant-based approaches are unable to support such scenarios due to the non-negligible delay induced by the handshake procedure for grant acquisition [4].

As a promising solution to this problem, *grant-free* random access schemes such as grant-free non-orthogonal multiple access (GF-NOMA) in which the base station (BS) does not exclusively assign radio resources to active users for data transmission have attracted significant attention [4], [5]. In a GF-NOMA system, each active user can directly transmit its packet to the BS without waiting for permission; as a result, however, the BS must cope with active user detection (AUD) to recover transmitted data accurately.

In this context, many approaches to accurate AUD have been investigated for synchronous GF-NOMA systems, where perfect synchronization between the BS and users in both time and frequency is assumed [6]–[14]. On the other hand, achieving ideal synchronization is impractical due to the nature of grant-free transmission, and AUD for asynchronous scenarios remains an ongoing research area [4]. In practice, due to practical limitations of crystal oscillators [15], the resulting carrier frequency offsets (CFOs) among the users degrade the performance.

To overcome this impediment, some approaches to AUD in the presence of CFOs have recently been proposed [16]–[20]. For instance, [16] proposed the block coordinate descent

(BCD)-based method for AUD and channel estimation (CE). In addition, [17] and [18] handled AUD using maximum likelihood estimation (MLE), which achieves higher accuracy than the BCD-based method of [16]. Meanwhile, since the MLE-based method uses a discrete approximation of the rotation caused by CFOs, the improvement of the performance requires the increase in the discretization size, resulting in high computational complexity. As an alternative, the approximate message passing (AMP)-based approaches for AUD and CE have been proposed in [19] and [20], assuming that the frequency error is limited to a certain range that meets standard requirements. Although they can perform AUD and CE efficiently, prior information such as *activity ratio* is necessary. This implies that a scheme to estimate prior information is required to achieve efficient AUD in the presence of CFOs.

For synchronous scenarios, schemes to estimate activity ratio, namely the number of active users, have been proposed [9], [11], [14]. Throughout this paper, this process is referred to as active user enumeration (AUE). In [9], the number of active users is estimated through rank estimation of the covariance matrix of the received pilot signal, to achieve precise AUD using the Riemannian optimization. However, this approach necessitates the eigenvalue decomposition of the received pilot signal and a sufficiently long pilot sequence, resulting in high computational complexity for AUE. On the other hand, [11] and [14] have proposed the AUE schemes using a very short common pilot sequence. The scheme in [11] uses a sequence orthogonal to the common sequence, while the scheme in [14] considers the MLE problem of the number of active users based on the covariance matrix of the received signal. These AUE schemes, utilizing a short common pilot, can estimate the number of active users with low complexity. However, since these AUE schemes use the pilot sequence, their estimation accuracy may degrade when CFO is present, similar to AUD.

To this end, in this letter, we propose two AUE schemes using a short common pilot sequence to estimate the number of active users in the presence of CFOs. Although the proposed schemes use the short common pilot as in [11] and [14], they do not rely on the orthogonality of the sequences or the formulation based on the *pure* pilot, both of which are affected by CFOs. Specifically, the proposed AUE schemes utilize the eigenvalues of the sample covariance matrix of the received signal, with one scheme designed for scenarios where the noise variance information is known, and the other for when it is unknown. Furthermore, the computational complexity for these schemes is comparable to that of conventional approaches. Numerical results demonstrate that the proposed AUE schemes achieve superior estimation accuracy compared to the conventional schemes proposed in [11] and [14].

This work has been submitted to the IEEE for possible publication. Copyright may be transferred without notice, after which this version may no longer be accessible. This work was partially supported by JSPS KAKENHI Grant Number JP23K13337 and Telecommunications Advancement Foundation Research Grant. T. Hara is with the Department of Electrical Engineering, Tokyo University of Science, Chiba 278-8510, Japan (email: t.hara@ieee.org).

Notation: The transpose and conjugate transpose are denoted by $(\cdot)^T$ and $(\cdot)^H$, respectively. The l_p -norm of a vector is expressed as $\|\cdot\|_p$. $\Re\{\cdot\}$ and $(\cdot)^*$ denote the real part and conjugate of the argument, respectively. In addition, $\mathbf{0}_L$ and \mathbf{I}_L denote the L -dimensional column vectors in which all elements are zeros and the $L \times L$ identity matrix, respectively. The determinant and trace of a square matrix \mathbf{A} are denoted by $|\mathbf{A}|$ and $\text{tr}(\mathbf{A})$. The expectation operator and operation that rounds x to the nearest integer are represented by $\mathbb{E}[\cdot]$ and $\lfloor x \rfloor$, respectively. $\mathbf{a} \circ \mathbf{b}$ denotes the element-wise product of two vectors \mathbf{a} and \mathbf{b} . Finally, $\mathcal{CN}(\boldsymbol{\mu}, \boldsymbol{\Sigma})$ represents a multivariate complex Gaussian distribution with mean $\boldsymbol{\mu}$ and covariance $\boldsymbol{\Sigma}$.

II. SYSTEM MODEL

We consider an uplink GF-NOMA system comprising N single antenna users and a common BS equipped with M antennas. At each coherence time, only $K \ll N$ users are active to transmit the packets including the same pilot used for estimating K at the BS. In this paper, we use $\mathbf{s} = [1 \ 1]^T$ as the same pilot. Furthermore, each user is assumed to be equipped with a low-cost crystal oscillator, which results in the CFO between the users and the common BS. Thus, the angular frequency between user n and the BS is modeled as $\omega_n \triangleq 2\pi\epsilon_n = 2\pi\Delta f_n T_s$, where ϵ_n , Δf_n , and T_s are the normalized CFO, the frequency offset in Hz, and the sampling period, respectively. We assume that $\epsilon_n \in [-\epsilon_{\max}, \epsilon_{\max}]$, where ϵ_{\max} denotes the maximum normalized CFO [19].

Let $\mathbf{Y} \in \mathbb{C}^{2 \times M}$ denote the received pilot signal at the BS. Then, the received signal can be written as

$$\begin{aligned} \mathbf{Y} &= \sum_{n \in \mathcal{A}} \sqrt{\beta_n \rho_n} (\mathbf{s} \circ \boldsymbol{\tau}(\omega_n)) \mathbf{h}_n^T + \mathbf{Z} \\ &= \sum_{n \in \mathcal{A}} \sqrt{\beta_n \rho_n} \boldsymbol{\tau}(\omega_n) \mathbf{h}_n^T + \mathbf{Z}, \end{aligned} \quad (1)$$

where $\boldsymbol{\tau}(\omega_n) = [1 \ e^{j\omega_n}]^T \in \mathbb{C}^{2 \times 1}$ is the phase rotation vector due to ω_n , and $\mathcal{A} \subset \{1, 2, \dots, N\}$, whose cardinality is K , is the set of active users. In addition, $\mathbf{h}_n \sim \mathcal{CN}(\mathbf{0}_M, \mathbf{I}_M)$ and $\mathbf{Z} \in \mathbb{C}^{2 \times M}$ denote the small-scale fading channel vector between user n and BS, and the noise matrix whose each entry follows an independently and identically distributed (i.i.d.) complex Gaussian distribution with zero mean and variance σ_z^2 , respectively. ρ_n and β_n denote the transmit power of user n and the large-scale fading component between user n and the BS. Throughout this paper, each active user is assumed to compensate for the effect of the large-scale fading component by the uplink power control, i.e., $\beta_n \rho_n = 1$ [11]. Thus, the received pilot signal model can be simplified as

$$\mathbf{Y} = \sum_{n \in \mathcal{A}} \boldsymbol{\tau}(\omega_n) \mathbf{h}_n^T + \mathbf{Z}. \quad (2)$$

Our goal is to estimate the number of active users, K , from the received pilot signal taking the effect of CFOs into account.

III. CONVENTIONAL AUE SCHEMES

In this section, to clarify the difference between conventional and proposed AUE schemes, we review the AUE schemes proposed in [11] and [14]. These conventional

schemes operate under the assumption that the probability function of \mathbf{Y} given K , \mathbf{s} , and $\omega_n = 0, \forall n$, is given by

$$p(\mathbf{Y}|K, \mathbf{s}) = \frac{1}{|\pi \boldsymbol{\Sigma}|^M} \prod_{m=1}^M \exp\left(-\mathbf{y}_m^H \boldsymbol{\Sigma}^{-1} \mathbf{y}_m\right), \quad (3)$$

where $\boldsymbol{\Sigma} = \mathbb{E}[\mathbf{y}_m \mathbf{y}_m^H] = K \mathbf{s} \mathbf{s}^H + \sigma_z^2 \mathbf{I}_2$. Thus, this assumption does not consider the effect of CFOs.

The AUE scheme in [11] utilizes the sequence $\mathbf{s}_\perp \in \mathbb{C}^{2 \times 1}$ that is orthogonal to \mathbf{s} and satisfies $\|\mathbf{s}_\perp\|_2 = \|\mathbf{s}\|_2$. Let $\mathbf{R} \triangleq \mathbf{Y} \mathbf{Y}^H / M \in \mathbb{C}^{2 \times 2}$ be the sample covariance matrix of the received pilot signal in (2). Then, the criterion to estimate K in [11] can be expressed as

$$\hat{K}_{\text{orth}} = \left\lfloor \frac{\mathbf{s}^H \mathbf{R} \mathbf{s}}{\|\mathbf{s}\|_2^4} - \frac{\mathbf{s}_\perp^H \mathbf{R} \mathbf{s}_\perp}{\|\mathbf{s}_\perp\|_2^2 \|\mathbf{s}\|_2^2} \right\rfloor. \quad (4)$$

When $\|\mathbf{s}\|_2 = \|\mathbf{s}_\perp\|_2 = 1$, (4) is equivalent to [11, eq. (5)]. It is worth noting that this scheme does not require the knowledge of noise variance σ_z^2 .

On the other hand, the AUE scheme in [14] considers the MLE problem of K . This problem can be formulated as

$$\underset{K \in [0, N]}{\text{minimize}} \quad \log |\boldsymbol{\Sigma}| + \text{tr}(\boldsymbol{\Sigma}^{-1} \mathbf{R}) \quad (5)$$

The solution of the optimization problem can be obtained by

$$\hat{K}_{\text{MLE}} = \left\lfloor \frac{\mathbf{s}^H \mathbf{R} \mathbf{s}}{\|\mathbf{s}\|_2^4} - \frac{\sigma_z^2}{\|\mathbf{s}\|_2^2} \right\rfloor. \quad (6)$$

As is obvious from (6), the estimation of K in [14] does not rely on \mathbf{s}_\perp , while it requires σ_z^2 .

IV. PROPOSED AUE SCHEMES

In this section, we propose two AUE schemes, named *Eig-sum* and *Eig-diff*, which utilize the eigenvalues of the sample covariance matrix \mathbf{R} , λ_{\max} and λ_{\min} ($< \lambda_{\max}$).

A. Preliminaries

The proposed schemes consider the covariance matrix of \mathbf{y}_m given ω_n for $n \in \mathcal{A}$, i.e.,

$$\begin{aligned} \tilde{\boldsymbol{\Sigma}} &= \mathbb{E}[\mathbf{y}_m \mathbf{y}_m^H] = \sum_{n \in \mathcal{A}} \boldsymbol{\tau}(\omega_n) \boldsymbol{\tau}(\omega_n)^H + \sigma_z^2 \mathbf{I}_2 \\ &= \begin{bmatrix} K + \sigma_z^2 & \sum_{n \in \mathcal{A}} e^{-j\omega_n} \\ \sum_{n \in \mathcal{A}} e^{j\omega_n} & K + \sigma_z^2 \end{bmatrix} \end{aligned} \quad (7)$$

The eigenvalues of this covariance matrix are given by

$$\Lambda_{\max} = K + \sigma_z^2 + \gamma, \quad (8)$$

$$\Lambda_{\min} = K + \sigma_z^2 - \gamma, \quad (9)$$

where

$$\gamma = \sqrt{\left(\sum_{n \in \mathcal{A}} e^{j\omega_n} \right) \left(\sum_{n \in \mathcal{A}} e^{-j\omega_n} \right)}. \quad (10)$$

Assuming K is sufficiently large, γ can be approximated as

$$\begin{aligned} \gamma &= K \sqrt{\left(\frac{1}{K} \sum_{n \in \mathcal{A}} e^{j\omega_n} \right) \left(\frac{1}{K} \sum_{n \in \mathcal{A}} e^{-j\omega_n} \right)} \\ &\approx K \sqrt{\mathbb{E}[e^{j\omega}] \mathbb{E}[e^{-j\omega}]}, \end{aligned} \quad (11)$$

where ω represents a random variable that takes values within the interval $[-2\pi\epsilon_{\max}, 2\pi\epsilon_{\max}]$. $\mathbb{E}[e^{j\omega}]$ in (11) is the characteristic function of ω .

B. Eig-sum: Proposed AUE With Knowledge of σ_z^2

As is obvious from (8) and (9), K can ideally be obtained based on the sum of the eigenvalues of $\tilde{\mathbf{Z}}$, i.e., $K = (\Lambda_{\max} + \Lambda_{\min})/2 - \sigma_z^2$, if the information of σ_z^2 is available at the BS. Following this fact, Eig-sum obtains the estimate of K by

$$\hat{K}_{\text{sum}} = \left\lfloor \frac{\lambda_{\max} + \lambda_{\min}}{2} - \sigma_z^2 \right\rfloor. \quad (12)$$

Since this scheme is based on the calculation to offset the term including CFOs, γ , it is expected to be robust against CFOs.

As in [11], we consider the normalized root mean-squared error (NRMSE) of this scheme, which is defined as

$$\text{NRMSE} = \frac{1}{K} \sqrt{\mathbb{E}[(\hat{K} - K)^2]}, \quad (13)$$

where \hat{K} is the estimate of the number of active users K . Given $\alpha = \mathbb{E}[e^{j\omega}]$, the NRMSE of Eig-sum can be obtained by

$$\text{NRMSE} = \frac{1}{K} \sqrt{\frac{K + K(K-1)\alpha^2 + (K + \sigma_z^2)^2}{2M}}. \quad (14)$$

For the derivation of (14), please refer to Appendix.

C. Eig-diff: Proposed AUE Without Knowledge of σ_z^2

Since $\mathbb{E}[e^{j\omega}]$ is an even function, $\mathbb{E}[e^{-j\omega}] = \mathbb{E}[e^{j\omega}]$ is satisfied.¹ Then, (11) can be written as

$$\gamma \approx K |\mathbb{E}[e^{j\omega}]|. \quad (15)$$

Furthermore, since $\Lambda_{\max} - \Lambda_{\min} = 2\gamma$, we can obtain the estimate of the number of active users, as follows:

$$\hat{K}_{\text{diff}} = \left\lfloor \frac{\lambda_{\max} - \lambda_{\min}}{2|\mathbb{E}[e^{j\omega}]|} \right\rfloor. \quad (16)$$

This scheme relies solely on the knowledge of ϵ_{\max} , which is usually available as the frequency errors of uplink users are confined within a certain range specified by the standard.

Note that, since the analysis of the NRMSE of Eig-diff is very complicated, this is left for future work.

D. Complexity Comparison

In this subsection, we discuss the computational complexity required for the proposed and conventional AUE schemes. Here, we express the entries of \mathbf{R} , as follows:

$$\mathbf{R} \triangleq \begin{bmatrix} R_1 & \tilde{R} \\ \tilde{R}^* & R_2 \end{bmatrix} = \begin{bmatrix} \frac{\|\mathbf{y}_1\|_2^2}{M} & \frac{\mathbf{y}_1 \mathbf{y}_2^H}{M} \\ \left(\frac{\mathbf{y}_1 \mathbf{y}_2^H}{M}\right)^* & \frac{\|\mathbf{y}_2\|_2^2}{M} \end{bmatrix}, \quad (17)$$

¹In the literature, CFO is often modeled as a random variable that follows a symmetric distribution, such as a uniform or Gaussian distribution. Hence, the characteristic function of ω is real-valued and even.

TABLE I
COMPUTATIONAL COMPLEXITY OF AUE SCHEMES.

AUE scheme		Number of multiplications
Eig-sum:	$\frac{R_1 + R_2}{2} - \sigma_z^2$	$2M + 3$
Eig-diff:	$\frac{\sqrt{(R_1 - R_2)^2 + 4\tilde{R}\tilde{R}^*}}{2\mathbb{E}[e^{j\omega}]}$	$3M + 7$
Orthogonal [11]:	$\Re\{\tilde{R}\}$	$M + 1$
MLE [14]:	$\frac{R_1 + R_2 + 2\Re\{\tilde{R}\}}{4} - \frac{\sigma_z^2}{2}$	$3M + 5$

TABLE II
SIMULATION PARAMETERS.

Number of potential users N	100
Number of active users K	25
Number of antennas at the BS M	32
Maximum normalized CFO ϵ_{\max}	0.15
Distribution of ω_n	Uniform distribution: $\omega_n \in [-2\pi\epsilon_{\max}, 2\pi\epsilon_{\max}]$
SNR $1/\sigma_z^2$	10 [dB]

where $\mathbf{y}_1 \in \mathbb{C}^{1 \times M}$ and $\mathbf{y}_2 \in \mathbb{C}^{1 \times M}$ represent the first and second rows of the received signal \mathbf{Y} , respectively. Then, \mathbf{y}_1 and \mathbf{y}_2 are given by

$$\mathbf{y}_1 = \sum_{n \in \mathcal{A}} \mathbf{h}_n^T + \mathbf{z}_1, \quad \mathbf{y}_2 = \sum_{n \in \mathcal{A}} e^{j\omega_n} \mathbf{h}_n^T + \mathbf{z}_2, \quad (18)$$

where $\mathbf{z}_1 \in \mathbb{C}^{1 \times M}$ and $\mathbf{z}_2 \in \mathbb{C}^{1 \times M}$ are the first and second rows of the noise matrix \mathbf{Z} .

Given $\mathbf{s} = [1 \ 1]^T$ and $\mathbf{s}_{\perp} = [1 \ -1]^T$, the computational complexity of AUE schemes can be summarized in TABLE I. This table also includes the equations for AUE schemes, which are expressed with R_1 , R_2 , and \tilde{R} ; however, their derivations are omitted owing to space constraints. This analysis is based on the fact that R_1 , R_2 , and \tilde{R} can be computed using the inner product of two M -dimensional vectors, while ignoring constant terms that can be predetermined, such as those involving σ_z^2 or $\mathbb{E}[e^{j\omega}]$. From TABLE I, Orthogonal [11] has the lowest complexity, whereas Eig-sum exhibits lower complexity than MLE [14]. Moreover, the complexity of Eig-diff is slightly higher than, but comparable to, that of MLE [14]. Therefore, the proposed AUE schemes exhibit computational complexity comparable to that of existing schemes.

V. NUMERICAL RESULTS

In this section, we investigate the performance of the proposed schemes through computer simulations. The simulation setup basically follows TABLE II unless otherwise specified. To assess the accuracy of AUE, we evaluate the NRMSE performance, which is defined by (13). In the simulations, we compare the following methods:

- *Eig-sum*: the proposed scheme given by (12).
- *Eig-diff*: the proposed scheme given by (16).
- *Orthogonal*: the AUE scheme in [11] given by (4).
- *MLE*: the AUE scheme in [14] given by (6).

The signal-to-noise ratio (SNR) is defined as $1/\sigma_z^2$. In addition, all simulation results include the analyzed NRMSE of Eig-sum in (14) as ‘‘Eig-sum (theory).’’

Fig. 1 shows the NRMSE performance as a function of ϵ_{\max} for $M = 32$ and $M = 128$. Figs. 1(a) and 1(b) show the

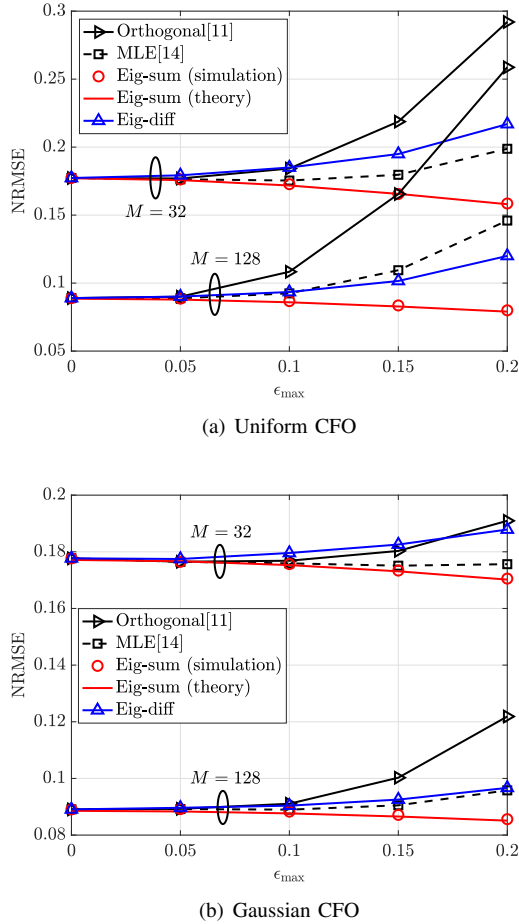


Fig. 1. NRMSE performance versus ϵ_{\max} .

performance for uniform CFO and Gaussian CFO² cases, respectively. As seen in Figs. 1(a) and 1(b), Eig-sum outperforms the other schemes, while Orthogonal performs worse than all the others, especially when ϵ_{\max} is large. Interestingly, the performance of Eig-sum slightly improves as ϵ_{\max} increases. This improvement is presumed to be due to the decrease in γ caused by the increase in ϵ_{\max} . Furthermore, the analyzed NRMSE aligns with the simulated NRMSE. We can also see that the performance of Eig-diff is superior to or comparable to that of MLE when $M = 128$, despite not using σ_z^2 . This is because Eig-diff considers the effect of CFOs in the covariance matrix of the received signal, making it more robust.

In Fig. 2, we show the NRMSE performance when the number of antennas M varies from 16 to 128. Similar to Fig. 1, this figure demonstrates that Eig-diff performs comparably to MLE when M is sufficiently large. Moreover, it turns out that Eig-sum consistently outperforms the other schemes.

Next, we examine the effect of the noise variance σ_z^2 in the AUE. Fig. 3 shows the NRMSE performance versus SNR. As seen in the figure, the relationship among the performances of all AUE schemes does not vary across all SNR. Given that the

²In this case, ω_n follows the Gaussian distribution with mean zero and standard deviation $2\pi\epsilon_{\max}/3$, in which about 99.7% of the values lie within $[-2\pi\epsilon_{\max}, 2\pi\epsilon_{\max}]$.

NRMSE of Eig-sum remains nearly constant with changes in SNR, especially in the high SNR region, it is reasonable to presume that the NRMSE of other methods would similarly remain largely unaffected by SNR variations.

Finally, Fig. 4 shows the NRMSE performance versus the number of active users K . This result indicates that the estimation error of the proposed schemes remains roughly constant under different value of K , similar to the conventional schemes. In light of the above, we can conclude that the proposed schemes are robust to both CFOs and the number of active users.

VI. CONCLUSION

In this letter, we proposed two AUE schemes for GF-NOMA in the presence of CFOs. Both proposed schemes utilize the eigenvalues of the sample covariance matrix of the received signal, with one scheme designed to function without requiring noise variance information. Numerical results demonstrate that the proposed schemes outperform conventional methods when the noise variance is known. Moreover, even without knowledge of the noise variance, our schemes perform comparably to these conventional approaches. Although this study focuses on a scenario with CFOs, addressing timing offsets is also necessary and is therefore left for future work.

APPENDIX

The NRMSE of Eig-sum can be calculated by (19), which is based on $\hat{K}_{\text{sum}} = \lfloor (R_1 + R_2)/2 - \sigma_z^2 \rfloor$. Note that the derivation of (14) ignores the rounding operation as in [11].

We first consider $\mathbb{E}[R_1]$, $\mathbb{E}[R_2]$, $\mathbb{E}[R_1^2]$, and $\mathbb{E}[R_2^2]$. Since \mathbf{y}_1 and \mathbf{y}_2 can be regarded as a random vector that follows $\mathcal{CN}(\mathbf{0}_M, (K + \sigma_z^2)\mathbf{I}_M)$, R_1 and R_2 follow the Erlang distribution with the shape parameter M and rate parameter $M/(K + \sigma_z^2)$. The mean and variance of this distribution are $K + \sigma_z^2$ and $(K + \sigma_z^2)^2/M$, respectively. Consequently, we can obtain the following relationships.

$$\mathbb{E}[R_1] = \mathbb{E}[R_2] = K + \sigma_z^2, \quad (20)$$

$$\mathbb{E}[R_1^2] = \mathbb{E}[R_2^2] = \left(1 + \frac{1}{M}\right) (K + \sigma_z^2)^2. \quad (21)$$

Next, we discuss the value of $\mathbb{E}[R_1 R_2]$. R_1 and R_2 can be expanded as follows:

$$\begin{aligned} R_1 &= \sum_{n \in \mathcal{A}} \frac{\|\mathbf{h}_n\|_2^2}{M} + \sum_{n \in \mathcal{A}} \sum_{n' \in \mathcal{A}, n' \neq n} \frac{\mathbf{h}_n^T \mathbf{h}_{n'}}{M} \\ &+ \sum_{n \in \mathcal{A}} \frac{\mathbf{h}_n^T \mathbf{z}_1}{M} + \sum_{n \in \mathcal{A}} \frac{\mathbf{z}_1^T \mathbf{h}_n}{M} + \frac{\|\mathbf{z}_1\|_2^2}{M}, \quad (22) \\ R_2 &= \sum_{n \in \mathcal{A}} \frac{\|\mathbf{h}_n\|_2^2}{M} + \sum_{n \in \mathcal{A}} \sum_{n' \in \mathcal{A}, n' \neq n} \frac{e^{j(\omega_n - \omega_{n'})} \mathbf{h}_n^T \mathbf{h}_{n'}}{M} \\ &+ \sum_{n \in \mathcal{A}} \frac{e^{j\omega_n} \mathbf{h}_n^T \mathbf{z}_2}{M} + \sum_{n \in \mathcal{A}} \frac{e^{-j\omega_n} \mathbf{z}_2^T \mathbf{h}_n}{M} + \frac{\|\mathbf{z}_2\|_2^2}{M}. \quad (23) \end{aligned}$$

Given that \mathbf{h}_n , ω_n , \mathbf{z}_1 , and \mathbf{z}_2 are independent of each other, $R_1 R_2$ can be expressed by (24) without including negligible terms, where we use the following relationship:

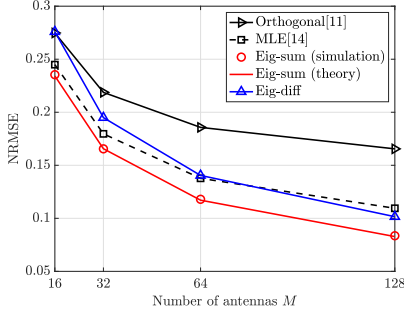
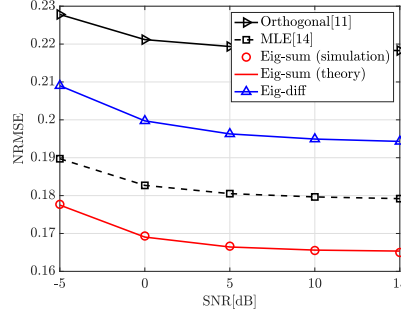
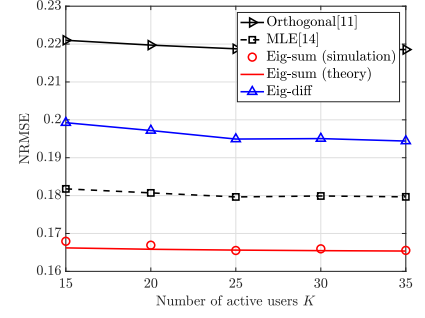
Fig. 2. NRMSE performance versus M .

Fig. 3. NRMSE performance versus SNR.

Fig. 4. NRMSE performance versus K .

$$\sum_{n \in \mathcal{A}} \sum_{n' \in \mathcal{A}, n' \neq n} \frac{\mathbf{h}_n^T \mathbf{h}_{n'}^*}{M} = \sum_{n \in \mathcal{A}} \sum_{n' \in \mathcal{A}, n' \neq n} \frac{\mathbf{h}_n^T \mathbf{h}_{n'}^*}{M}. \quad (25)$$

In addition, since $\mathbf{h}_n \sim \mathcal{CN}(\mathbf{0}_M, \mathbf{I}_M)$, $\mathbf{z}_1 \sim \mathcal{CN}(\mathbf{0}_M, \sigma_z^2 \mathbf{I}_M)$, and $\mathbf{z}_2 \sim \mathcal{CN}(\mathbf{0}_M, \sigma_z^2 \mathbf{I}_M)$, we can obtain the relationships: $\mathbb{E}[\|\mathbf{h}_n\|_2^4] = M + M^2$, $\mathbb{E}[\|\mathbf{h}_n\|_2^2] = M$, $\mathbb{E}[\mathbf{h}_n^* \mathbf{h}_n^T] = \mathbf{I}_M$, and $\mathbb{E}[\|\mathbf{z}_1\|_2^2] = \mathbb{E}[\|\mathbf{z}_2\|_2^2] = M\sigma_z^2$. As a result, $\mathbb{E}[R_1 R_2]$ can be calculated by

$$\mathbb{E}[R_1 R_2] = \frac{K + K(K-1)\alpha^2}{M} + (K + \sigma_z^2)^2. \quad (26)$$

In light of the above, by substituting (20), (21), and (26) into (19), we can derive (14).

REFERENCES

- [1] N. H. Mahmood, H. Alves, O. A. López, M. Shehab, D. P. M. Osorio, and M. Latva-Aho, "Six key features of machine type communication in 6G," in *Proc. 2020 2nd 6G Wireless Summit*, Levi, Finland, Mar. 2020, pp. 1–5.
- [2] Y. Wu, X. Gao, S. Zhou, W. Yang, Y. Polyanskiy, and G. Caire, "Massive access for future wireless communication systems," *IEEE Wireless Commun.*, vol. 27, no. 4, pp. 148–156, Aug. 2020.
- [3] X. Chen, D. W. K. Ng, W. Yu, E. G. Larsson, N. Al-Dahir, and R. Schober, "Massive access for 5G and beyond," *IEEE J. Sel. Areas Commun.*, vol. 39, no. 3, pp. 615–637, Mar. 2021.
- [4] M. B. Shahab, R. Abbas, M. Shirvanimoghaddam, and S. J. Johnson, "Grant-free non-orthogonal multiple access for IoT: A survey," *IEEE Commun. Surveys Tuts.*, vol. 22, no. 3, pp. 1805–1838, 3rd Quart. 2020.
- [5] L. Liu, E. G. Larsson, W. Yu, P. Popovski, C. Stefanovic, and E. de Carvalho, "Sparse signal processing for grant-free massive connectivity: A future paradigm for random access protocols in the internet of things," *IEEE Signal Process. Mag.*, vol. 35, no. 5, pp. 88–99, Sep. 2018.
- [6] S. Haghghatshoar, P. Jung, and G. Caire, "Improved scaling law for activity detection in massive MIMO systems," in *Proc. IEEE Int. Symp. Inf. Theory*, Vail, CO, USA, Jun. 2018, pp. 381–385.
- [7] L. Liu and W. Yu, "Massive connectivity with massive MIMO—Part I: Device activity detection and channel estimation," *IEEE Trans. Signal Process.*, vol. 66, no. 11, pp. 2933–2946, Jun. 2018.
- [8] K. Senel and E. G. Larsson, "Grant-free massive MTC-enabled massive MIMO: A compressive sensing approach," *IEEE Trans. Commun.*, vol. 66, no. 12, pp. 6164–6175, Dec. 2018.
- [9] X. Shao, X. Chen, and R. Jia, "A dimension reduction-based joint activity detection and channel estimation algorithm for massive access," *IEEE Trans. Signal Process.*, vol. 68, pp. 420–435, Dec. 2019.
- [10] M. Ke, Z. Gao, Y. Wu, X. Gao, and R. Schober, "Compressive sensing-based adaptive active user detection and channel estimation: Massive access meets massive MIMO," *IEEE Trans. Signal Process.*, vol. 68, pp. 764–779, Jan. 2020.
- [11] H. Han, Y. Li, W. Zhai, and L. Qian, "A grant-free random access scheme for mMTC communication in massive MIMO systems," vol. 7, no. 4, pp. 3602–1462, Apr. 2020.
- [12] H. Iimori, T. Takahashi, K. Ishibashi, G. T. F. de Abreu, and W. Yu, "Grant-free access via bilinear inference for cell-free MIMO with low-coherence pilots," *IEEE Trans. Wireless Commun.*, vol. 20, no. 11, pp. 7694–7710, Nov. 2021.
- [13] T. Hara and K. Ishibashi, "Blind multiple measurement vector AMP based on expectation maximization for grant-free NOMA," vol. 11, no. 6, pp. 1201–1205, Jun. 2022.
- [14] M. Zhu, Y. Sun, L. You, Z. Wang, Y.-F. Liu, and S. Cui, "Rethinking grant-free protocol in mMTC," Apr. 2024. [Online]. Available: <https://arxiv.org/abs/2404.16152>
- [15] J. Xu, J. Yao, L. Wang, Z. Ming, K. Wu, and L. Chen, "Narrowband Internet of Things: Evolutions, technologies, and open issues," vol. 5, no. 3, pp. 1449–1462, Jun. 2018.
- [16] Y. Li, M. Xia, and Y.-C. Wu, "Activity detection for massive connectivity under frequency offsets via first-order algorithms," *IEEE Trans. Wireless Commun.*, vol. 18, no. 3, pp. 1988–2002, Mar. 2019.
- [17] T. Hara, H. Iimori, and K. Ishibashi, "Activity detection for uplink grant-free NOMA in the presence of carrier frequency offsets," in *Proc. IEEE Int. Conf. Commun. Workshops*, Dublin, Ireland, Jun. 2020, pp. 1–6.
- [18] W. Liu, Y. Cui, F. Yang, L. Ding, J. Xu, and X. Xu, "MLE-based device activity detection for grant-free massive access under frequency offsets," in *Proc. IEEE Int. Conf. Commun.*, Seoul, Korea, Republic of, May 2022, pp. 1629–1635.
- [19] G. Sun et al., "Massive grant-free OFDMA with timing and frequency offsets," *IEEE Trans. Wireless Commun.*, vol. 21, no. 5, pp. 3365–3380, May 2022.
- [20] K. Ueda, T. Hara, and K. Ishibashi, "Iterative activity detection and carrier frequency offset estimation for grant-free NOMA," in *Proc. IEEE 33rd Int. Symp. Pers., Indoor and Mobile Radio Commun.*, Kyoto, Japan, Sep. 2022, pp. 1–6.

$$\text{NRMSE} = \frac{1}{K} \sqrt{\mathbb{E} \left[\left(\frac{R_1 + R_2}{2} - \sigma_z^2 \right)^2 \right]} - K^2 = \frac{1}{K} \sqrt{\frac{1}{4} \mathbb{E}[R_1^2] + \frac{1}{4} \mathbb{E}[R_2^2] + \frac{1}{2} \mathbb{E}[R_1 R_2] - \sigma_z^2 (\mathbb{E}[R_1] + \mathbb{E}[R_2]) + \sigma_z^4 - K^2}. \quad (19)$$

$$R_1 R_2 = \sum_{n \in \mathcal{A}} \frac{\|\mathbf{h}_n\|_2^4}{M^2} + \sum_{n \in \mathcal{A}} \sum_{n' \in \mathcal{A}, n' \neq n} \left(\frac{\|\mathbf{h}_n\|_2^2 \|\mathbf{h}_{n'}\|_2^2}{M^2} + e^{j(\omega_n - \omega_{n'})} \frac{\mathbf{h}_n^T \mathbf{h}_{n'}^* \mathbf{h}_n^T \mathbf{h}_{n'}^*}{M^2} \right) + \frac{\|\mathbf{z}_1\|_2^2 + \|\mathbf{z}_2\|_2^2}{M^2} \sum_{n \in \mathcal{A}} \|\mathbf{h}_n\|_2^2 + \frac{\|\mathbf{z}_1\|_2^2 \|\mathbf{z}_2\|_2^2}{M^2}. \quad (24)$$